Sensitivity of elevated temperature load carrying capacity of thin-walled steel members to local imperfections

C. Maraveas, T. Gernay & J.M. Franssen
Fire Safety Unit, ArGEnCo Dept., University of Liege, Belgium

ABSTRACT: The local buckling capacity of fire exposed thin-walled steel cross sections is affected by the reduction in strength and stiffness due to elevated temperatures and by the amplitude of the initial local imperfections. Several researchers have proposed design methods to calculate the capacity of these steel members at elevated temperatures, but they used different methodologies and different amplitude of local imperfections in the extensive numerical analyses that are typically at the base of these methods. This variability in hypotheses happens because there is no clear provision defining the local imperfection amplitude for fire design in the codes (European or US). EN 1993-1-5 proposes amplitude values of local imperfections for ambient temperature design, while EN 1090-2 defines a - different- maximum allowed size of fabrication tolerance during production. Meanwhile, other sizes of local imperfections have also been proposed in the literature, with values different than those from EN 1993-1-5 and EN 1090-2. This paper reviews the existing code provisions and compares the existing design models and their assumptions for thin-walled steel cross sections. Finite element analyses are then conducted on isolated steel plates at elevated temperatures to investigate the effect of local imperfections. Finally, specific amplitude of local imperfections is proposed for fire design of thin-walled steel members.

1 INTRODUCTION

The use of slender steel sections, i.e. sections made of thin steel plates, has increased in recent years because they provide excellent strength to weight ratio; this trend has also been favored by the development of higher steel grades. Yet, a major issue with slender sections is local buckling that may occur in zones subjected to compression: in the flange under compression for elements in bending and in the web for elements in compression. In very deep sections, shear can also trigger local buckling in the web if it is too slender.

Furthermore, past fire accidents have demonstrated local buckling failures in structural members with slender cross sections, like in WTC 5 (MacAllister, 2008) and Broadgate fire (Wang, 2002).

To take local instabilities into account, several design methods have been proposed by researchers based on finite element analyses of isolated plates (Couto et al, 2014, Couto et al, 2015, Franssen et al, 2014, Quiel et al, 2010) or analytical methods (Knobloch et al, 2006). As the current codes do not include a specific method for the calculation of the capacity of such structural members at elevated temperatures, the ambient temperature methods of EN 1993-1-5, 2006 and AISC, 2005 can be used in conjunction with elevated temperature material models from EN 1993-1-2, 2005 or AISC, 2005 respectively. A comparison of the plate capacity predicted by different proposed models, whether based on design codes or numerical analyses, is showed in Figure 1. The horizontal axis on the plot is the elevated temperature plate slenderness (Eq. 13) and the vertical axis is the strength reduction due to local buckling. Although these models give similar trends, the discrepancy in quantitative results is significant with a ratio in

the order of 2 between the extremes. Table 1 shows the governing parameters (i.e. assumptions) used in the models based on numerical analyses. The parameters a, b and t are the length, width and thickness of the plate, respectively. It can be seen that different authors assumed different values for these parameters, which naturally lead to different results. Furthermore, other researchers are using amplitude of imperfections even different from those of Table 1 (e.g. Saif et al, 2013). The results are affected by the amplitude of the initial local imperfections, by the geometry of the local imperfections (number of half-waves) and by the dimensions of the plate (ratio a/b) (Gerald et al, 1957). The effect of the number of half-waves and a/b ratio is discussed in another study (Maraveas et al, 2017). This paper presents an investigation on the influence of the amplitude of the initial imperfections. Considering code and standard provisions, the literature and new numerical results of simulations on isolated plates, recommendations are made for the amplitude of imperfection to be used for the design of slender plates at elevated temperature.

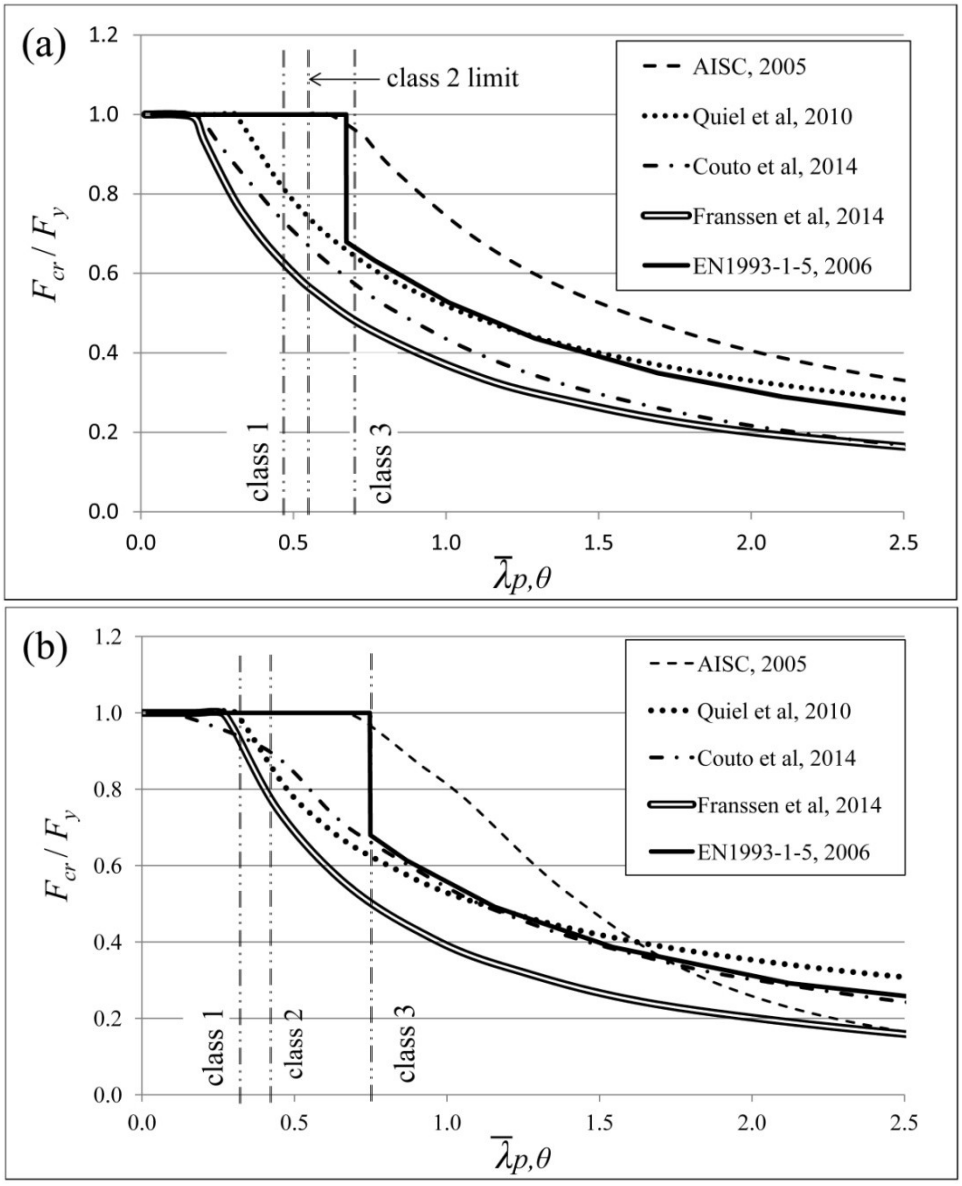

Figure 1. Comparison of proposed design and code methods for capacity of slender plates at 500 ^{o}C, (a) for stiffened plates (web) and (b) for unstiffened plates (flange).

Table 1. Governing analysis parameters used in the numerical simulations by different authors.

Reference	a/b	Number ofhalf-waves	Amplitude of imperfections
Franssen et al, 2014	flange: 2 web: 1	1	flange: b/50 = 0.020 b web: b/200 = 0.005 b
Couto et al, 2014	4	flange: 1, web: 4	flange: 80% b/50 = 0.016 b web: 80% b/100 = 0.008 b
Quiel et al, 2010	5	flange: 3, web: 5	flange: 0.156 t web: 0.100 t

2 CODE AND STANDARD PROVISIONS

2.1 *EN 1993-1-5*

EN 1993-1-5 defines the amplitude of local imperfections that must be included in FE models. These imperfections should include both geometric and structural imperfections. Two alternatives are allowed: considering explicitly the two types of imperfections; or utilizing equivalent geometric imperfections. In the former case, it is mentioned that "*geometric imperfections may be based on the shape of the critical plate buckling modes with amplitudes equivalent to 80% of the geometric fabrication tolerances.*" Structural imperfections should be represented by residual stresses. On the other hand, in the latter case, a table is proposed for equivalent geometric imperfections. For the type of plates relevant for this study on slender structural members (flanges and web), the amplitude of the equivalent local imperfections is defined as minimum(a/200, b/200) where a and b are the dimensions of the panel or the subpanel (Fig. 2b).

2.2 *EN 1090-2: Manufacturing tolerance of plated members*

EN 1090-2 defines the essential manufacturing tolerances as the maximum acceptable tolerances to satisfy the design assumptions for structures in terms of resistance and stability, whereas it defines functional manufacturing tolerances as the ones which might be required to meet a function other than resistance and stability, like fit up or appearance. The essential manufacturing tolerances are given in Eq. (1) and (2).

$$\text{Web curvature/distortion: } max \begin{cases} \min \begin{cases} \begin{cases} b'/t \le 80, & b'/200 \\ 80 < b'/t \le 200, & b'^2/(16000t) \\ b'/t > 200, & b'/80 \end{cases} \\ b'/100 \end{cases} \\ t \end{cases} \tag{1}$$

$$\text{Flange distortion: } \begin{cases} b'/t \le 20, & b'/150 \\ b'/t > 20, & b'^2/(3000t) \end{cases} \tag{2}$$

where b' is the total flange width or the web height (Fig. 2a). Eq. (2) permits high essential manufacturing tolerances for slender cross sections (b'/t > 20), as shown by Figure 3. Also, Eq. (1) gives for most slender cross section a maximum fabrication tolerance equal to the thickness t of the plate.

The functional manufacturing tolerances for execution classes 1 and 2 are given by Eq. (3) and (4):

$$\text{Web curvature and distortion: for Class 1 } max \begin{cases} b'/100 \\ 5\ mm \end{cases} \text{ and for Class 2 } max \begin{cases} b'/150 \\ 3\ mm \end{cases} \tag{3}$$

Flange distortion: for Class 1, b'/100 and, for Class 2, b'/150 (4)

The standard does not specify functional manufacturing tolerances for execution classes 3 and 4. It can be assumed that tolerances lower than given by Eq. (3) and (4) are permitted for execution classes 3 and 4 as these classes correspond to important structures (Consequence Class 3 per EN 1990, 2002).

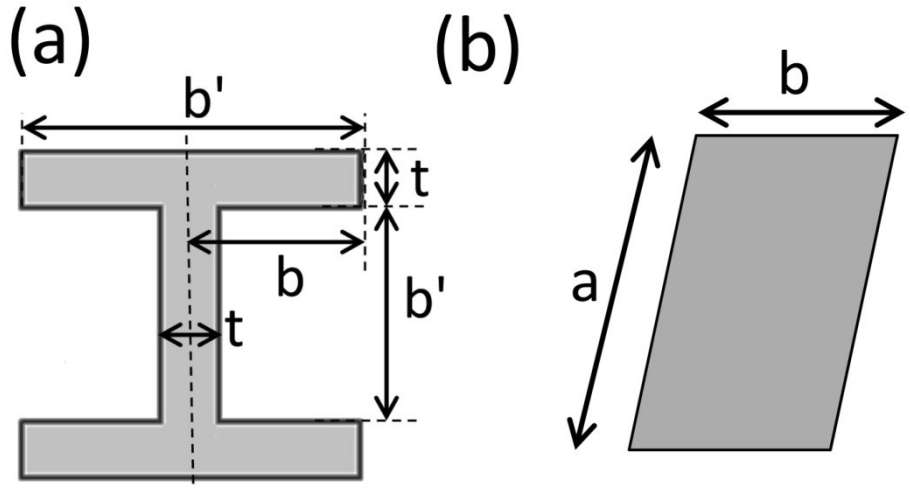

Figure 2. Definition of (a) b, b' and t for I or H cross-sections and (b) a and b for isolated plate.

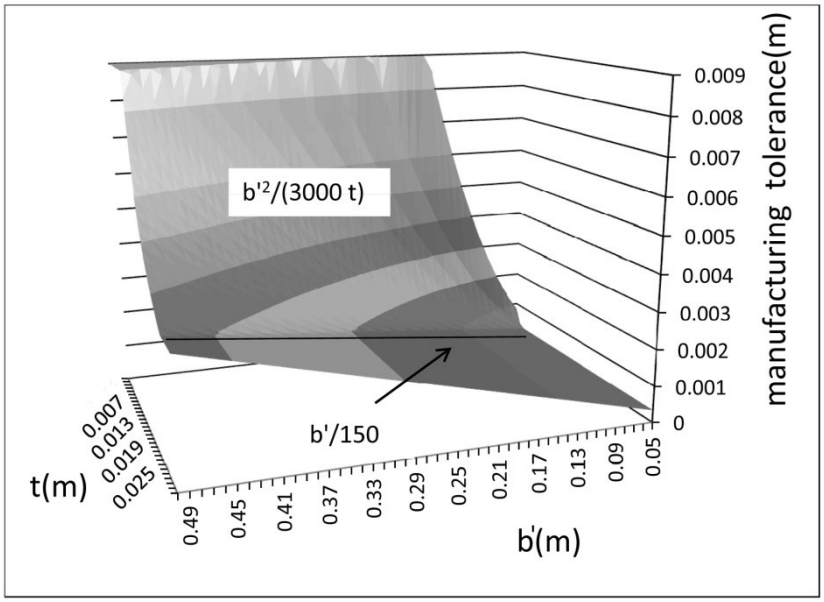

Figure 3. Flange essential manufacturing tolerances according to EN1090-2, 2008.

2.3 *Geometric imperfection amplitude as 80% of the manufacturing tolerance*

According to EN 1993-1-5, 2006, the amplitude of geometric imperfections can be calculated as 80% of the manufacturing tolerances. So, the geometric imperfection amplitude is given by Eq. (5) and (6) directly derived from Eq. (1) and (2):

$$\text{Web curvature/distortion: } max^{\min}_{0.8\,t}\left\{\begin{cases} b'/t \le 80, & b'/250 \\ 80 < b'/t \le 200, & b'^2/(20000t) \\ b'/t > 200, & b'/100 \end{cases}\right. \quad b'/125 \tag{5}$$

Flange distortion: $\begin{cases} b/t \leq 10, & b/93.75 \\ b/t > 10, & b^2/(937.5\ t) \end{cases}$ (6)

where b and b' are defined in Fig. 2a. These values can be taken as local geometric imperfections in the model. Note that, in this case, it is necessary to also use residual stresses in the model to represent the structural imperfections.

2.4 *EN 10034 – EN 10279: Manufacturing tolerance of hot rolled sections*

Slender hot rolled sections are sensitive to local buckling during fire too. EN 10034, 1993 defines the maximum tolerances for I and H sections (for k = k' and 50% for half flange, see Table 2 of EN 10034, 1993):

Flange: b' > 110 mm, 0.5% of b' and maximum 1.65 mm (7)

Web: $\begin{cases} \text{where t} < 40 \text{ mm} & \begin{cases} b' \leq 110\ mm & 2.5\ mm \\ 110\ mm < b' \leq 325 mm & 3.5\ mm \\ b' > 325\ mm & 5\ mm \end{cases} \\ \text{where t} \geq 40 \text{ mm} & \begin{cases} 110\ mm < b' \leq 325 mm & 5.0\ mm \\ b' > 325\ mm & 8.0\ mm \end{cases} \end{cases}$ (8)

Similarly, EN 10279, 2000 defines the tolerance for hot rolled channels as:

Flange: b > 100 mm, 1.25% of b (9)

Web: $\begin{cases} h \leq 100\ mm & 0.5\ mm \\ 100\ mm < h \leq 200 mm & 1.0\ mm \\ h > 200\ mm & 1.5\ mm \end{cases}$ (10)

where h is the height of the cross section.

Comparing the manufacturing tolerances of hot rolled sections (Eq. (7) to (10)) with those of EN 1090-2, 2008 (Eq. (1) and (2)), the maximum allowed manufacturing tolerances for the web are similar but the hot rolled sections have lower permitted manufacturing tolerances for the flange when the cross section is slender.

2.5 *Summary of code requirements for local imperfections*

Working in the European framework, one option is to use the equivalent geometric imperfections with amplitude defined as min(a/200, b/200) for flange and web plates, where a and b are the dimensions of the panel or the subpanel. Another option is to base the geometric imperfection on the manufacturing tolerance, and to also include in the analysis residual stresses for the structural imperfection. In the latter case, high geometric imperfections can be obtained for slender plates, see Figure 3. Besides, the question of residual stresses has to be addressed.

At ambient temperatures, these two methods from EN 1993-1-5 are giving very different results in terms of imperfection amplitude. The method combining imperfections as a function of manufacturing tolerance and residual stresses is unfavorable comparing with the equivalent imperfections method. Indeed, the amplitude of imperfections calculated by the first method (80% of tolerance) is always higher than the amplitude calculated according to the equivalent method. Furthermore, the residual stresses are reducing further the strength of the plate, when they are combined with the unfavorable large imperfections. At elevated temperature, however, the effect of residual stresses has been shown to be very limited (FIDESC4, 2015), so that the difference between the two methods becomes a bit less significant.

In the next section, numerical simulations are conducted to investigate the effect of different local imperfection amplitudes. Residual stresses are not explicitly considered in these simulation, as it has been shown that their effect is very limited at elevated temperature (FIDESC4, 2015).

3 FINITE ELEMENT SIMULATIONS OF STEEL PLATES AT ELEVATED TEMPERATURES

In order to assess the effect of different local imperfection amplitudes, finite element analyses of isolated plates are performed using the nonlinear finite element software SAFIR® (Franssen, 2005). The methodology used for the analyses (for instance, the justification of the aspect ratio a/b, the number of half-waves, etc.) is described in details in Maraveas et al, 2017. The first model (Figure 4(a)) is simply supported at all 4 sides with a/b=1; it is simulating a stiffened plate (equivalent to a web). 400 shell elements are used after convergence verification (Figure 5). Imposed displacements are applied in the x direction at one side whereas the opposite side is restrained in the same direction. The lateral sides are free to expand in the y-direction, to allow unrestrained Poisson effect. The local imperfections are applied in one half-wave (m = n = 1) following the equation:

$$w(x,y) = w_o \sin\left(\frac{m\pi x}{a}\right) \sin\left(\frac{n\pi y}{b}\right) \tag{11}$$

where w_o is the local imperfection amplitude.

The second finite element model is unstiffened (equivalent to a flange), simply supported on three sides (Figure 4(b)), with aspect ratio a/b=5 and 2000 shell elements used after convergence verification. The local imperfections are applied in 4 half-waves (m = 4, n = 1) following the eq. 12.

$$w(x,y) = w_o \sin\left(\frac{m\pi x}{a}\right) \sin\left(\frac{n\pi y}{2b}\right) \tag{12}$$

In order to assess the effect of local imperfection amplitudes to plates of different slenderness, the thickness is modified to get different values of slenderness calculated according to eq. 13 from EN 1993-1-5, 2005:

$$\lambda_{p,\theta} = \frac{b/t}{28.4\varepsilon\sqrt{k_\sigma}} \tag{13}$$

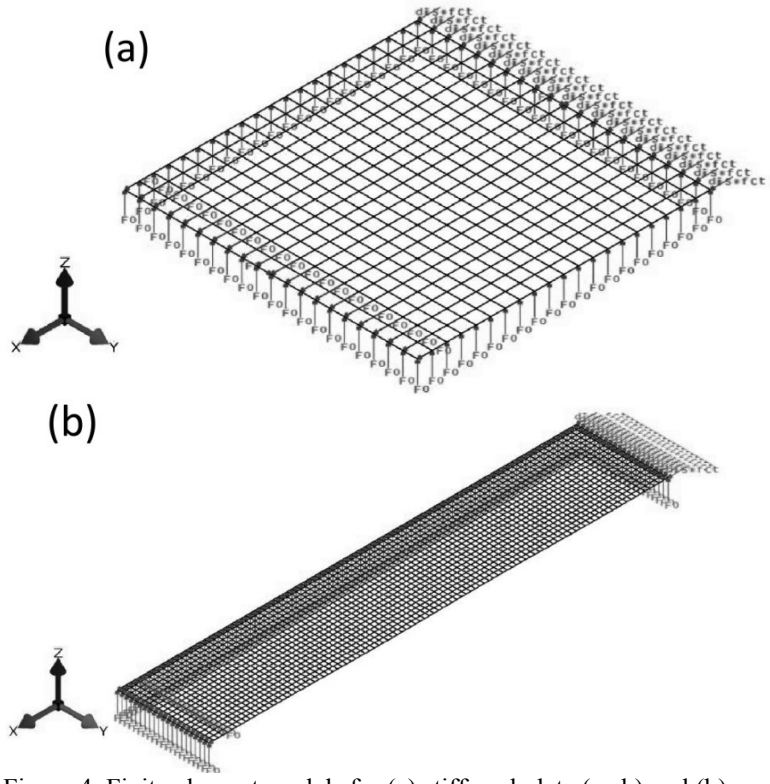

Figure 4. Finite element models for (a) stiffened plate (web) and (b) unstiffened plate (flange).

where k_σ is a factor considering the applied boundary conditions defined in EN 1993-1-5, 2005 and ε has been taken for elevated temperatures from the equation:

$$\varepsilon = \sqrt{\frac{k_{E,\theta}}{k_{y,\theta}}}\sqrt{\frac{235}{f_y}} \quad (14)$$

where $k_{E,\theta}$ and $k_{y,\theta}$ are the reduction factors of Young's modulus and yield strength respectively for temperature θ.
The yield strength considered 235 MPa for both plates.

4 NUMERICAL RESULTS

For the two types of studied plates (web and flange equivalent, see Figure 4), the failure mode corresponds to the pre-applied local imperfection geometry (Figure 6). This shows the importance of the geometry of the plate and the geometry of imperfection, which are discussed in more details in Maraveas et al., 2017.

The analysis results are presented in Figure 7 for the flange and in Figure 8 for the web. Two different slenderness are considered for each type of plate, in order to assess the effect of local imperfection amplitude of thick plates ($\bar{\lambda}_{p,\theta}$ = 1.5 for flange and $\bar{\lambda}_{p,\theta}$ = 1.0 for web) and slender plates ($\bar{\lambda}_{p,\theta}$ = 3.0 for flange and $\bar{\lambda}_{p,\theta}$ = 2.0 for web). The results show the effect of local imperfections ranging from b/2000 to 20 mm. Different intermediate values of geometric imperfections discussed in Section 2 are represented on the plot. The results are plotted for ambient temperature and for a temperature of 550°C.

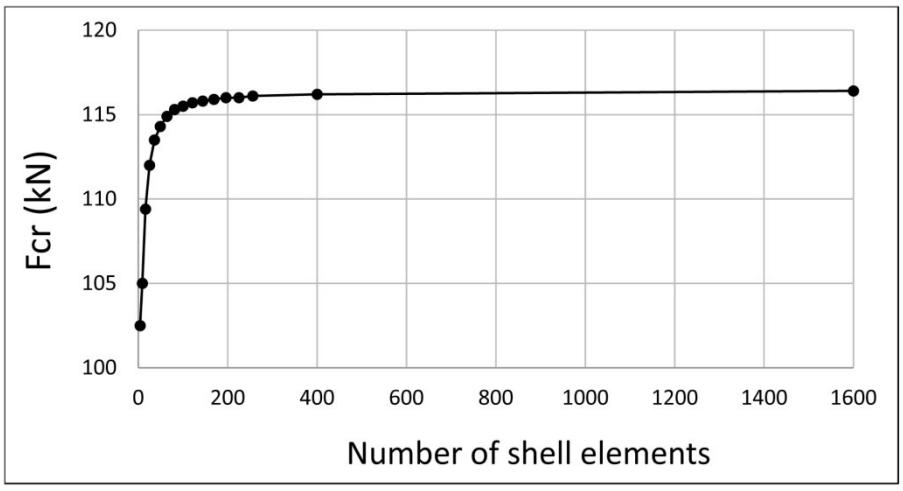

Figure 5. Convergence verification for square plate with a = b = 0.4 m under axial compression.

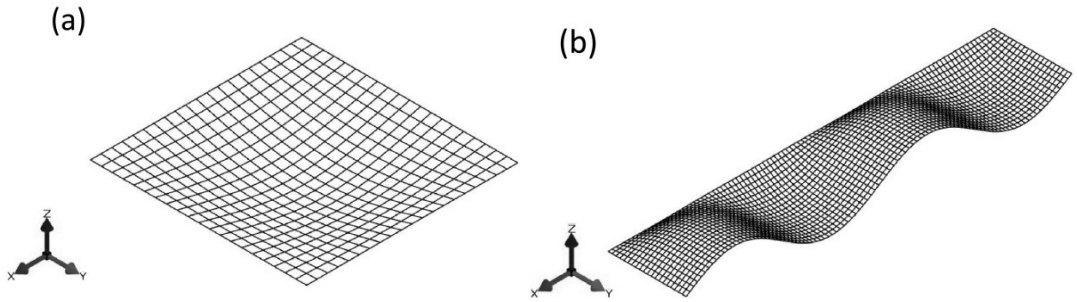

Figure 6. Failure modes of (a) four sides simply supported plate (web) and (b) three sides simply supported plate (flange).

The results show that the amplitude of local imperfections has an influence on the computed capacity of slender plates in compression. The computed capacity varies by more than 25% for the range of amplitudes studied here. However, the effect of the amplitude of local imperfections becomes limited when the amplitude exceeds a value of b/100. For the flanges, in Figure 7(a), the difference in terms of critical load is 10% between the equivalent local imperfection amplitude b/200 (equivalent value as defined in EN1993-1-5) and the limit value given by Eq.

(6) (geometric imperfection based on manufacturing tolerances). In Figure 7(b), the equivalent difference increases to 13%, as Eq. (6) is giving high local imperfection amplitudes for slender flanges.

For the web, in Figure 8(a) the difference in terms of critical load is 9.3% between b/200 and Eq. (5) amplitudes. For the slender web, in Figure 8(b), the same difference is just 1.7%.

The effect of the amplitude of local imperfections seems to be qualitatively the same at ambient and at elevated temperature. However, this effect is quantitatively less significant at elevated temperature.

As discussed in a companion paper (Maraveas et al, 2017), the effect of the geometry of local imperfection (number of half-waves) and the geometry of the plate (ratio a/b) can affect the critical load by up to 50%. So, the effect of these parameters is higher than that of the amplitude of imperfections.

For these reasons, it seems reasonable to adopt a recommendation for the amplitude of imperfection at elevated temperature that is similar to the one at ambient temperature.

From Fig. (7) and (8), it can be clearly seen that the amplitude of the equivalent geometric imperfections (hence including implicitly the residual stresses, according to EN 1993-1-5) is actually smaller than the amplitude of the geometric imperfections based on manufacturing tolerance, to which the structural imperfections still have to be added according to the code. This seems illogical since, reasonably, the structural imperfections (represented by residual stresses), are expected to have a detrimental effect on the plate capacity.

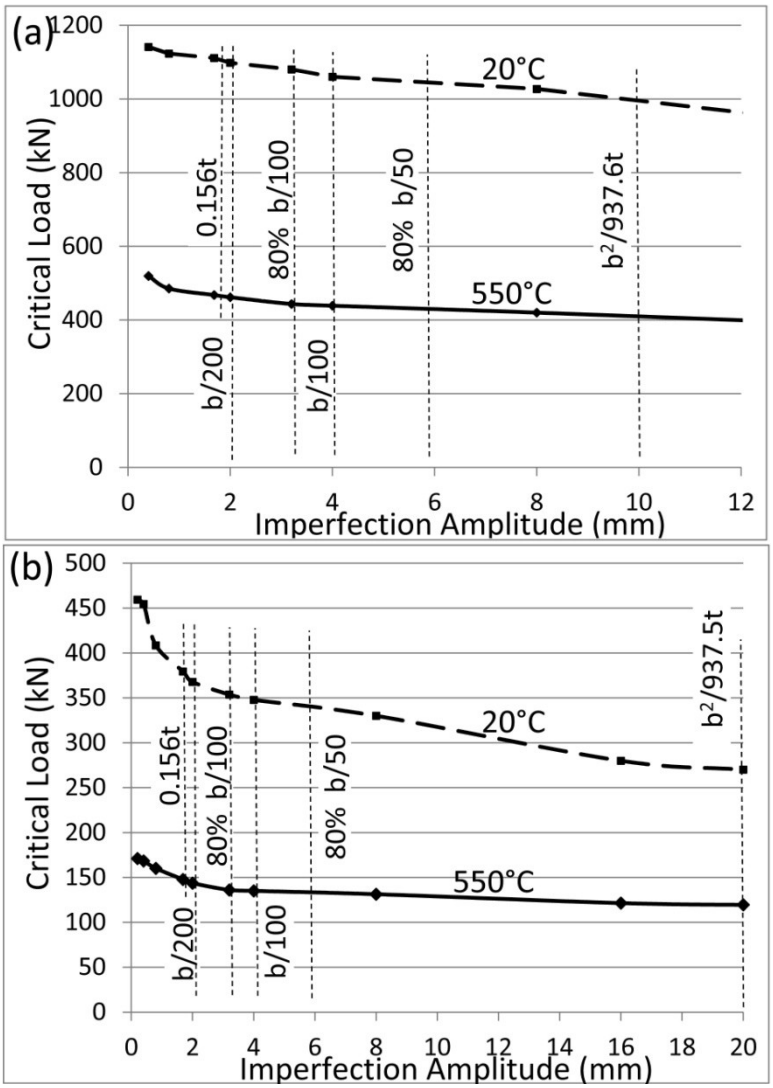

Fig. 7 Critical load vs local imperfection amplitude for three sides simply supported plates with (a) $\bar{\lambda}_{p,\theta} = 1.5$ and (b) $\bar{\lambda}_{p,\theta} = 3.0$ at 20 °C and 550 °C.

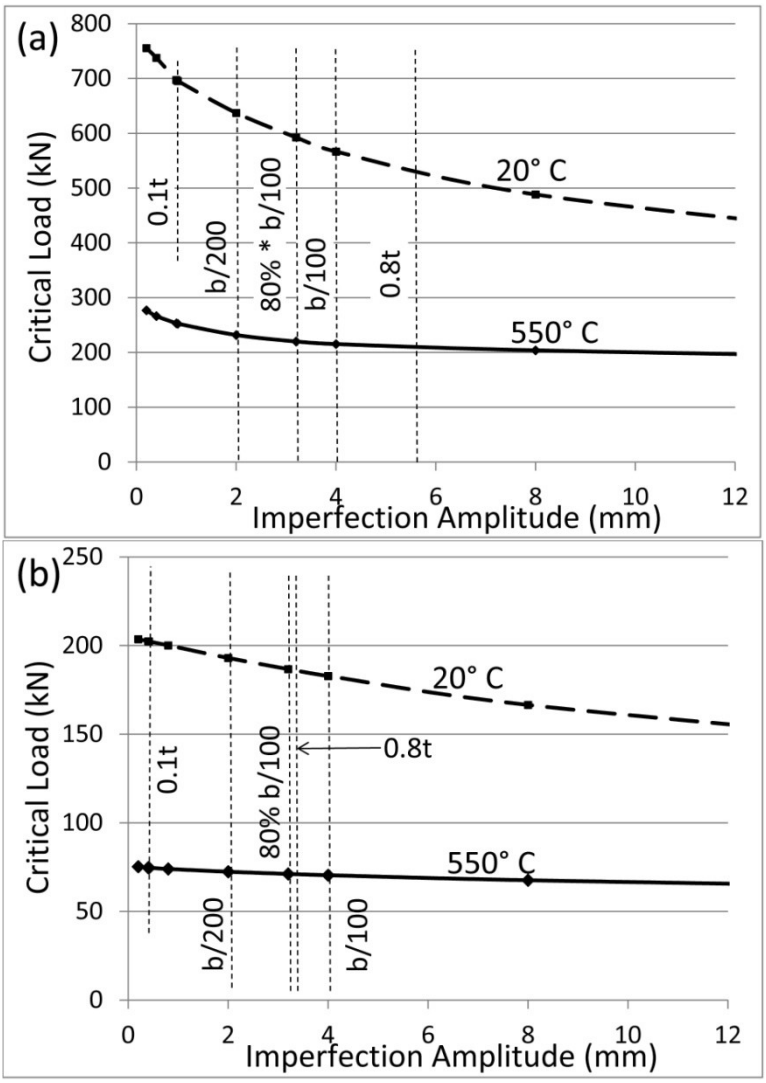

Fig. 8 Critical load vs local imperfection amplitude for four sides simply supported plates with (a) $\bar{\lambda}_{p,\theta} = 1.0$ and (b) $\bar{\lambda}_{p,\theta} = 2.0$ at 20 °C and 550 °C.

5 CONCLUSIONS

Considering the previous information and analysis results, the below conclusions can be drawn:

- The fire design codes such as EN 1993-1-2, 2005 do not provide any information regarding the amplitude of local imperfections.
- The standard code EN 1993-1-5, 2006 (for ambient temperature) proposes the use of equivalent local imperfections or the use of a combination of geometric imperfections, based on manufacturing tolerances, and residual stresses.
- Results of numerical analyses by finite element method on slender plates at elevated temperatures show that the amplitude of local imperfections affects the critical load. However, the effect is less significant than for other parameters such as the number of half-waves and the aspect ratio (Maraveas et al., 2017).
- The effect of the amplitude of local imperfections becomes less significant when this amplitude exceeds a b/100 limit, which can be derived from manufacturing tolerances. Also, the difference in results obtained following the two approaches of EN1993-1-5 is – generally – less than 10%. Note that the effect of residual stresses has not been considered in this study. Furthermore, the effect of the imperfection amplitude at elevated temperature is less significant than at ambient temperatures.

- As a conclusion, it is proposed to adopt the equivalent local imperfection amplitude per EN 1993-1-5, 2006 (which here corresponds to: min(a/200,b/200)) and to use it for studies at elevated temperature. This definition of the amplitude has the merit of being simple, of incorporating implicitly the residual stresses, and being consistent with the approach of ambient temperature. This local imperfection amplitude must be applied to the most unfavorable critical buckling shape of the plate and the most unfavorable plate geometry as it is defined in Maraveas et al, 2017.

6 ACKNOWLEDGEMENTS

This research was supported by the University of Liege and the EU in the context of the FP7-PEOPLE-COFUND-BeIPD project.

REFERENCES

AISC, 2005. Steel construction manual, 13th ed. American Institute of Steel Construction.

Couto, C., Real, P.V., Lopes, N., Zhao, B., 2015. Resistance of steel cross-sections with local buckling at elevated temperatures, Constructional Steel Research, 109, p. 101-104.

Couto, C., Real, P.V., Lopes, N., Zhao, B., 2014. Effective width method to account for the local buckling of steel thin plates at elevated temperatures, Thin-Walled Structures, 84, p. 134-149.

EN 10034, 1993.Structural steel I and H sections. Tolerances on shape and dimensions, European Committee for Standardisation.

EN1090-2, 2008. Execution of steel structures and aluminium structures – part 2: technical requirements for steel structures. European Committee for Standardisation.

EN 10279, 2000. Hot rolled steel channels. Tolerances on shape, dimension and mass, European Committee for Standardisation.

EN 1990, 2002. Eurocode: Basis of structural design. Brussels: European Committee for Standardisation.

EN 1993-1-2, 2005. Eurocode 3: design of steel structures — part 1–2: general rules —structural fire design. Brussels: European Committee for Standardisation.

EN 1993-1-5, 2006. Eurocode 3 — design of steel structures — part 1-5: plated structural elements. Brussels: European Committee for Standardisation.

FIDESC4, 2015, Fire design of steel members with welded or hot-rolled class 4 cross-sections, Final report, Research program of the Research Fund for Coal and Steel.

Franssen, J.M., Cowez, B., Gernay, T., 2014. Effective stress method to be used in beam finite elements to take local instabilities into account. Fire Safety Science 11, 544-557. 10.3801/IAFSS.FSS.11-544

Franssen, J.-M., 2005. SAFIR, A thermal/Structural Program for Modelling Structures under Fire, Eng J A.I.S.C., 42, p. 143-158.

Franssen, J.-M., Gernay, T. 2017. Modeling structures in fire with SAFIR®: Theoretical background and capabilities, Journal of Structural Fire Engineering, 8(3).

Gerald, G, Backer, H. Buckling of Flat Plates, NACA Technical Note 3781, USA, 1957.

Knobloch, M., Fontana, M., 2006. Strain-based approach to local buckling of steel sections subjected to fire. Constructional Steel Research, 62, p. 44-67.

Maraveas, C., Gernay, T., Franssen, J.M., 2017. Buckling of steel plates at elevated temperatures: Theory of perfect plates vs Finite Element Analysis, 2nd International Conference on Structural Safety Under Fire and Blast Loading – CONFAB, London, UK.

McAllister, T., 2008. Federal building and fire safety investigation of the World Trade Center disaster: structural fire response and probable collapse sequence of World Trade Center building 7. Gaitherburg. MD, National Institute of Standards and Technology [NIST NCSTAR 1-9].

Quiel, S.E., Garlock, M.E.M., 2010. Calculating the buckling strength of steel plates exposed to fire, Thin-Walled Structures, 48, p. 684-695.

Seif, M., McAllister, T., 2013. Stability of wide flange structural steel columns at elevated temperatures, Constructional Steel Research, 84, p. 17-26.

Wang, Y.C., 2002. Steel and composite structures: behaviour and design for fire safety, CRC Press, London.